Thermodynamic Analysis of the Structural Stability of the Tetrameric Oligomerization Domain of p53 Tumor Suppressor†

Craig R. Johnson,‡ Paul E. Morin,§ Cheryl H. Arrowsmith,§ and Ernesto Freire*,‡

Department of Biology and Biocalorimetry Center, The Johns Hopkins University, Baltimore, Maryland 21218, and Division of Molecular and Structural Biology, Ontario Cancer Institute, and Department of Medical Biophysics, University of Toronto, 500 Sherbourne Street, Toronto, Ontario M4X 1K9, Canada

Received January 23, 1995; Revised Manuscript Received March 7, 1995⊗

ABSTRACT: The structural stability of an amino acid fragment containing the oligomerization domain (residues 303−366) of the tumor suppressor p53 has been studied using high-precision differential scanning calorimetry (DSC) and circular dichroism spectroscopy (CD). Previous NMR solution structural determinations have revealed that the fragment forms a symmetric 29.8 kDa tetramer composed of a dimer of dimers (p53tet) [Lee, W., Harvey, T. S., Yin, Y., Yau, P., Litchfield, D., & Arrowsmith, C. H. (1994) *Nature Struct. Biol. 1,* 877−890]. Thermal unfolding of the tetramer is reversible and can be described as a two-state transition in which the folded tetramer is converted directly to unfolded monomers ($N_4 \leftrightarrow 4U$). According to the DSC and CD data, the population of intermediate species consisting of folded monomers or dimers is insignificant, indicating that isolated dimeric or monomeric structures have a much lower stability than the dimer and do not become populated during thermal denaturation under the conditions studied. The transition temperature of unfolding is found to be highly dependent on protein concentration and to follow the expected behavior for a tetramer that dissociates upon unfolding. Experiments conducted at pH 4.0 in 25 mM sodium acetate at a tetramer concentration of 145.8 μM have a transition temperature (T_m) of 75.3 °C while at 0.5 μM the value drops to 39.2 °C. The enthalpy change of unfolding at 60 °C is 26 kcal (mol of monomer)$^{-1}$ with a heat capacity change of 387 cal (K·mol of monomer)$^{-1}$. The stability of p53tet is dependent on pH and salt concentration. Decreasing the pH from 7.0 to 3.0 lowered the stability of the tetramer significantly (T_m's of 84.5 and 34.3 °C, respectively) while higher salt concentrations increased the stability, especially at low pH values. The results of these studies indicate that the tetramer is stabilized primarily by intersubunit interactions rather than intrasubunit interactions. In fact, more than 58% of the total area buried from the solvent in the folded tetramer corresponds to the intersubunit interfaces, and 70% of this area is hydrophobic. These results emphasize the role of quaternary structure in the stabilization of small oligomeric proteins.

The nucleoprotein p53 is the most commonly mutated protein found in human tumors (Hollstein et al., 1991; Levine et al., 1991; Lane, 1992; Vogelstein & Kuntzler, 1992; Donehower & Bradley, 1993; Harris, 1993). Believed to function as a transcription factor regulating genes responsible for arrest of cellular growth at G1/S phase, this molecule is made dysfunctional through deletions and mutations in just over 50% of human cancer tissues from which it has been sequenced. It has also been observed to form inactive complexes with many virally encoded oncogenes including those from human papilloma virus and SV40. Our present understanding allows the division of this 393 amino acid (aa) protein into five functional regions: (i) an acidic transactivation domain [aa 20−42 (Unger et al., 1992)], (ii) a DNA binding domain [aa 102−292 (Bargonetti et al., 1993; Halazonetis & Kandil, 1993; Pavletich et al., 1993; Cho et al., 1994)], (iii) a primary nuclear localization signal [aa 316−325 (Sturzbecher et al., 1992)], (iv) a tetramerization domain [aa 325−355 (Halazonetis & Kandil, 1993; Pavletich et al., 1993)], and (v) an apparent carboxy-terminal regulatory domain [aa 363−393 (Hupp et al., 1992)]. Detailed structural information describing the interaction and juxtaposition of these domains among one another has not yet been achieved for the intact 212 kDa protein. However, atomic level resolution structures have been obtained for the DNA binding and tetramerization domains in isolation (Cho et al., 1994; Clore et al., 1994; Lee et al., 1994). The 31 aa tetramerization domain forms a small compact dimer of dimers with three mutually perpendicular axes of 2-fold symmetry. The protein studied in this paper (p53tet) contains the entire tetramerization domain plus an additional 22 amino acids at the N terminus and 11 amino acids at the C terminus. According to the NMR data, these additional amino acids are mostly unstructured in solution and therefore are not expected to contribute significantly to the unfolding thermodynamics.

The tetramerization domain of this protein is of notable structural interest in that it is the smallest known protein homotetramer. NMR structural studies indicate that monomer−monomer interfaces are stabilized largely through hydrophobic interactions. NMR studies of different isotopically labeled protein (Lee et al., 1994) also showed that the subunits can be exchanged to form heterodimers, with the dimers exchanging at a faster rate than all four monomers.

† This work was supported by NIH Grants RR-04328, GM-37911, and NS-24520, the Cancer Research Society Inc., Montreal, Quebec, Canada, the Human Frontiers in Science Program, Strasbourg, France, and NATO-NSF Fellowship Award RCD-9255313 to P.E.M.

‡ The Johns Hopkins University.

§ University of Toronto.

⊗ Abstract published in *Advance ACS Abstracts,* April 1, 1995.

0006-2960/95/0434-5309$09.00/0

This suggested the possibility of a two-state unfolding mechanism. In this paper, we show that p53tet has a highly stable structure stabilized primarily by intersubunit interactions displaying a highly cooperative two-state thermal unfolding process.

MATERIALS AND METHODS

Protein Purification and Concentration Determination. Expression of recombinant protein was carried out using the expression vector pET-53tet (Lee et al., 1994), a pET-19b (Novogen, Madison, WI) derived T7 expression system. The pET-53tet expression plasmid encodes amino acids 303−366 of p53 preceded by a polyhistidine purification tag and an enterokinase cleavage site. *Escherichia coli* BL21(DE3) cotransformed with pET-53tet and pLys-S (Studier, 1991) was grown in 4−6 L batches of Luria broth at 37 °C and induced with 1 mM isopropyl thiogalactoside when shaken cultures reached an optical density of 0.65 at 600 nm. Cell pellets were lysed via freeze−thaw in the presence of lysis buffer (5 mM benzamidine, 5 mM imidazole, 20 mM Tris·HCl, pH 7.4), treated with DNase I and 10 mM $MgCl_2$, and then centrifuged at 25000*g*. Approximately 90% of overexpressed p53tet was found in the soluble fraction of the cell extract. The clarified cell extract was loaded onto a 4-mL bed of NTA Sepharose (Qiagen, Chatsworth, CA) equilibrated in 500 mM NaCl, 5 mM imidazole, and 20 mM Tris·HCl, pH 7.4, and washed with 100 mM imidazole, 500 mM NaCl, and 20 mM Tris·HCl, pH 7.4, until the optical density at 280 nm reached 0. p53tet was then eluted from the column by increasing the imidazole concentration to 0.5 M. SDS−PAGE showed a protein of 90% purity after this single purification step. The imidazole and NaCl concentrations were reduced to 100 mM each via stir-cell filtration (Amicon) and dilution. Enterokinase (Biozyme, San Diego, CA) was added in the presence of 5 mM $CaCl_2$, and proteolytic cleavage was allowed to progress at room temperature until completion as judged via visual inspection of SDS−PAGE gels (overnight). The cleaved mixture was then diluted 10-fold into 250 mM NaCl, 0 mM imidazole, and 20 mM Tris·HCl, pH 7.4, and loaded onto a fresh 4-mL NTA Sepharose column equilibrated in the same buffer. Under these conditions, all the protein bound to the column, and excess calcium was removed. The column buffer was then exchanged to 20 mM sodium phosphate, pH 7.4, and 250 mM NaCl. The cleaved protein product lacking the polyhistidine amino terminus was eluted by the stepwise addition of 60 mM imidazole to the column buffer. Uncleaved p53tet, cleaved polyhistidine fragments, and minor *E. coli* impurities with intrinsically high affinities for the NTA Sepharose present in the mixture prior to cleavage could then be eluted from the column with 0.5 M imidazole. The pH of the eluted sample was reduced to 7.0 by addition of HCl and the imidazole removed via stir-cell filtration/dilution or dialysis. The yield of purified protein was 10−12 mg/L of culture.

Prior to an experiment, samples were dialyzed for 14 h at 4 °C against 4 L of the appropriate buffer using Spectra/por 3000 molecular weight cutoff dialysis membrane. Peptide concentrations (per monomer) were determined using the calculated extinction coefficient $\epsilon_{280} = 1280\ M^{-1}\ cm^{-1}$ (Gill & von Hippel, 1989), which was verified by amino acid analysis.

Differential Scanning Calorimetry (DSC). Protein concentrations between 30.3 and 146 μM at various solution conditions were scanned at 1 °C min^{-1} using the newly developed series of high-precision differential scanning calorimeters DS-92 and DS-93 (Biocalorimetry Center, The Johns Hopkins University, Baltimore, MD). Both of these instruments are computer interfaced, allowing for automated instrument control and data collection. Samples and reference solutions were properly degassed and carefully loaded into the calorimeter to eliminate bubbling effects. Reproducibility of baselines was verified by multiple scans, and sample folding reversibility was monitored by scanning the samples twice. Absolute and excess heat capacities were analyzed using modifications of the nonlinear least squares fitting software developed in this laboratory as described before (Freire & Biltonen, 1978; Montgomery et al., 1993; Xie et al., 1995).

Circular Dichroism Spectroscopy (CD). CD experiments were conducted using the Jasco J-710 spectropolarimeter which is computer interfaced for automatic instrument control and data accumulation. Wavelength scans were performed with 2.5 μM tetramer in a 5-mm rectangular cell at a number of discrete temperatures ranging from 21.8 to 80.6 °C. For each distinct temperature, complete spectra were obtained by the average of five consecutive scans collected from 190 to 240 nm at 1-nm intervals. These experiments were conducted using a scan rate of 5 nm min^{-1}, a response time of 8 s per point, and a bandwidth of 1 nm. Buffer scans were accumulated and subtracted from the sample scans, and the mean residue ellipticity was computed. Temperature was controlled using a Haake F3 circulating water bath attached to a water-jacketed cell holder that surrounds the sample cell. The temperature was measured using a S/N117.C temperature probe connected to a Micro-therm 1006 thermometer (Hart Scientific).

CD temperature scans were performed using the time scan mode of the Jasco J-710 by scanning continuously as the temperature is varied from 10 to 80 °C at a rate of 1 °C min^{-1}. The mean ellipticity at 222 nm was recorded every 20 s with a response time of 0.5 s and a bandwidth of 1 nm. Temperature was controlled by a Haake PG 20 temperature programmer interfaced to the Haake F3 circulating water bath. The temperature of the jacketed sample cell was recorded at 5-min intervals, and the intervening ellipticity temperatures were interpolated to yield complete ellipticity vs temperature curves. The fraction of unfolded tetramer F_u was calculated from the ellipticity by the standard relationship

$$F_u = (\theta - \theta_N)/(\theta_U - \theta_N)$$

θ is the value of the ellipticity at any temperature. θ_N and θ_U represent the ellipticity values at temperatures where the fully folded and fully unfolded states exist, respectively. These values were obtained by performing linear regression on the baselines preceding and following the transition region.

RESULTS AND DISCUSSION

Calorimetric and CD Experiments. The thermal stability of p53tet was measured by high-sensitivity differential scanning calorimetry at a number of different pH and salt conditions. The transitions were reversible under all the

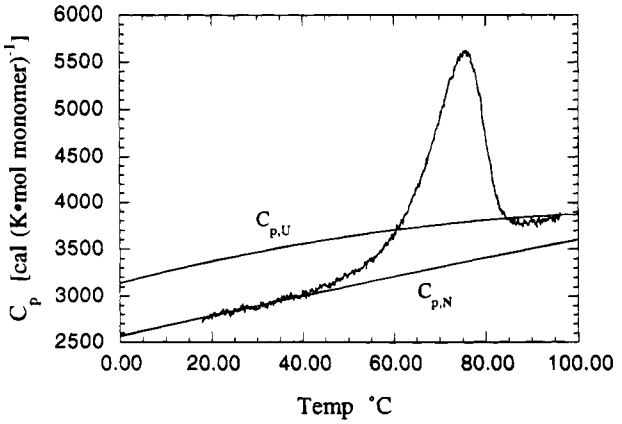

FIGURE 1: Partial molar heat capacity of p53tet as a function of temperature. The experiment was performed at pH 4.0 in 25 mM sodium acetate with a tetramer concentration of 146 μM. The solid lines represent the heat capacities of the native ($C_{p,N}$) and unfolded ($C_{p,U}$) states, respectively.

conditions studied as demonstrated by repeated scans of the same sample. Figure 1 shows the partial molar heat capacity function of a 146 μM tetramer solution at pH 4.0, 25 mM sodium acetate buffer. The figure illustrates the characteristic gradual linear increase in heat capacity of the native state at low temperature, the transition region, and the nonlinear increase characteristic of the unfolded state. At 25 °C, the heat capacity of the native state is 2.8 kcal (K•mol of monomer)$^{-1}$ or 0.38 cal (K•g)$^{-1}$, which is slightly higher than the mean value obtained for globular proteins [0.348 ± 0.005 cal (K•g)$^{-1}$] and consistent with the NMR observation that close to 30 amino acids per monomer are unstructured in the native state and therefore exhibit a higher degree of hydration. The heat capacity of the unfolded state is similar to the one expected from that of an unstructured polypeptide of the same amino acid composition (Makhatadze & Privalov, 1990; Freire, 1994; Gomez et al., 1995), indicating that the polypeptide chain is fully unfolded and hydrated after thermal denaturation.

Figure 2 displays a set of DSC scans obtained at protein concentrations of 70.5, 93.5 and 145.8 μM tetramer at pH 4.0 and 25 mM sodium acetate. In this figure, the excess heat capacity function obtained after subtraction of the heat capacity of the native state is shown. It is clear from the figure that the transition temperature increases with concentration, as expected for a system that undergoes dissociation upon unfolding (Freire, 1989). Transition curves at concentrations lower than those shown in the figure were examined by CD as the calorimetric response does not allow accurate measurements at lower concentrations. At the highest concentration studied the transition is characterized by a peak with a maximum at 75.3 °C, an enthalpy change (ΔH) of 32 kcal (mol of monomer)$^{-1}$, and an excess heat capacity difference between the native and denatured state of 390 cal (K•mol of monomer)$^{-1}$. (The thermodynamic parameters in this paper will all be given on a per mole of monomer basis unless otherwise noted.) It is also apparent that the transition curves are skewed to the low-temperature side of the transition as expected for an unfolding transition coupled to dissociation (Freire, 1989).

As mentioned above, circular dichroism spectroscopy (CD) was used to study the features of the transition at lower concentrations. Figure 3 displays a series of wavelength scans from 190 to 240 nm conducted at a number of different temperatures with a concentration of 2.5 μM tetramer. The curves are found to be well represented by a population-weighted linear combination of the pure component conformational spectra for α-helix, β-sheet, and random coil. The presence of a well-defined isodichroic point is consistent with a system having only two states. At low temperatures the structure is approximately 40% random coil with the remaining structure having both α-helical- and β-sheet-like character. This is consistent with the NMR and calorimetric data which indicate that approximately 30 amino acids per monomer are unstructured in the native state. As the temperature is increased, the proportion of α-helix and β-sheet decreases, eventually revealing only random coil.

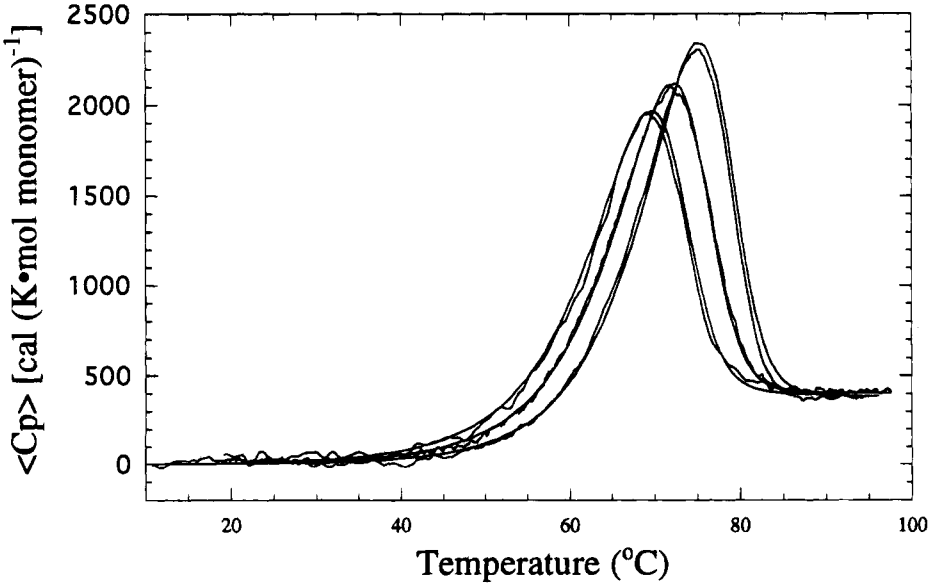

FIGURE 2: Excess heat capacity of p53tet as a function of protein concentration. Experiments were performed in 25 mM sodium acetate at pH 4.0. Tetramer concentrations are from left to right 70.5, 93.5, and 145.8 μM. Theoretical curves generated from the fitted parameters given in Table 1 are shown as solid lines along with their corresponding experimental data.

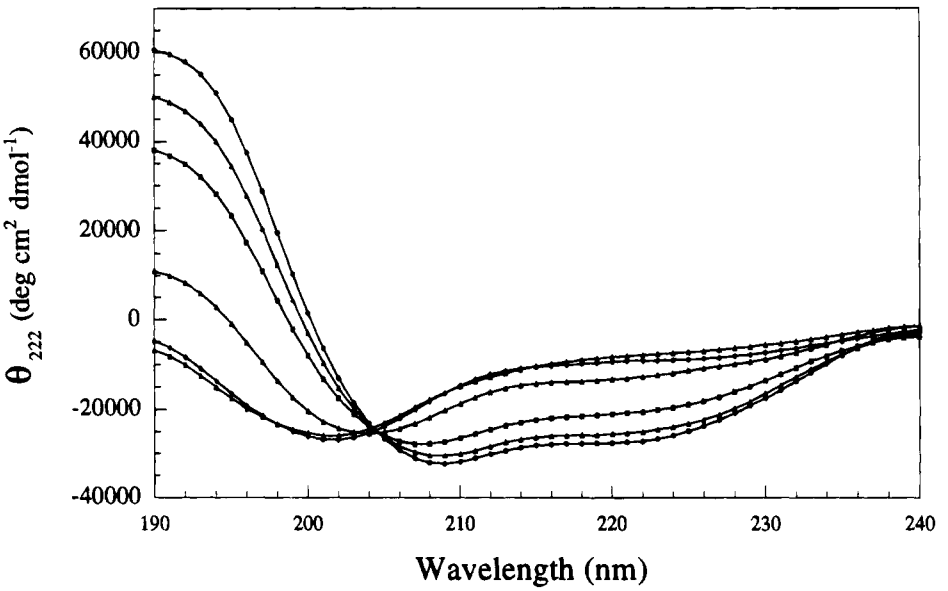

FIGURE 3: CD spectra of p53tet as a function of temperature. Experimental conditions are 2.5 μM tetramer in 25 mM sodium acetate at pH 4.0. Temperatures are from partially structured to unstructured 21.3, 39.3, 45.0, 51.1, 59.4, 70.4, and 80.6 °C.

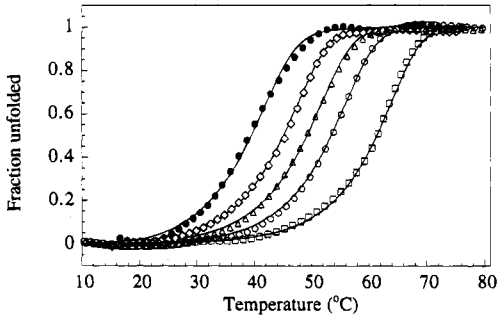

FIGURE 4: CD data showing the fraction of p53tet unfolded as a function of temperature at pH 4.0. Concentrations are from left to right 0.5 μM (filled circles), 1.25 μM (diamonds), 2.5 μM (triangles), 5 μM (open circles), and 20 μM (squares) tetramer. Ellipticity readings at 222 nm were monitored as the temperature was scanned up at a rate of 1 °C min^{-1}. For clarity the experimental data were smoothed using the Jasco J-710 software package with every fifth point being displayed. Theoretical curves generated from the thermodynamic parameters derived from the DSC data obtained at pH 4.0 (Table 1) are displayed as solid lines.

A second set of CD experiments were performed at a number of different concentrations ranging from 0.5 to 20 μM tetramer by scanning up in temperature while monitoring the ellipticity at 222 nm (Figure 4). This experimental procedure mimics the characteristics of the DSC experiments, allowing for fractional population determination at much lower concentrations. The low-temperature ellipticity values represent the native state of the protein. As the temperature increases, more of the protein is converted to the unfolded state and the ellipticity values rise. As with the DSC experiments, the transition temperature is seen to increase as the concentration of the protein is increased.

Statistical Thermodynamic Analysis. Two-state concentration-dependent self-associating thermal unfolding can be described using the tools of statistical thermodynamics (Thompson et al., 1993). In the case of p53tet we begin by describing the system in the simplest possible form, that of a folded tetramer (N_4) unfolding to four unfolded monomers (U) upon increasing temperature with no intermediate states. More complicated expressions can be developed in order to include intermediate species, but as is demonstrated here, those formulations were not necessary to explain the experimental data for p53tet. The folded tetramer/unfolded monomer equilibrium can be represented as

$$N_4 \rightleftharpoons 4U \tag{1}$$

where K is the equilibrium constant defined in the standard way as

$$K = [U]^4/[N_4] \tag{2}$$

The total protein monomer concentration (P_T) can be expressed as

$$P_T = 4[N_4] + [U] \tag{3}$$

The fractional population in the native (F_N) and unfolded (F_U) states is given by

$$F_N = 4[N_4]/P_T \tag{4}$$

$$F_U = [U]/P_T \tag{5}$$

Algebraic manipulation of expressions 2−5 results in the fourth-order equation.

$$F_U^4 + \frac{KF_U}{4P_T^3} - \frac{K}{4P_T^3} = 0 \tag{6}$$

The roots of this equation give the value of the fraction of molecules in the unfolded state as a function of the equilibrium constant and the total protein concentration. The value of the total protein concentration is known and by definition

$$K = \exp(-\Delta G°/RT) \tag{7}$$

where $\Delta G°$ is the intrinsic free energy of stabilization and can be defined in the standard way as

$$\Delta G° = \Delta H°(T°) + \Delta C_p(T - T°) - T[\Delta S°(T°) + \Delta C_p \ln(T/T°)] \tag{8}$$

Table 1: Thermodynamic Parameters of p53tet Unfolding as a Function of pH, Salt, and Tetramer Concentration

[NaCl] (mM)	buffer (25 mM)	pH	p53tet tetramer concn (μM)	T_m (°C)	$T°$ (°C)[a]	$\Delta H(T°)$ [kcal (mol of monomer)$^{-1}$]	$\Delta S(T°)$ [cal (K·mol of monomer)$^{-1}$]	$\Delta C_p(T°)$ [cal (K·mol of monomer)$^{-1}$]	SSR[b]
250	glycine	3.0	67.0	54.5	95.5	42.5	115.3	398	40.3
250	acetate	4.0	73.5	73.7	112.6	49.5	128.4	426	63.6
250	phosphate	6.0	30.3	82.9	123.6	52.0	131.1	398	128.1
250	phosphate	7.0	57.0	85.3	124.4	52.3	131.6	418	51.6
0	glycine	3.0	63.8	34.3	82.1	37.4	105.3	458	41.8
0	acetate	4.0	70.5	69.5	110.8	46.2	120.4	399	68.9
0	acetate	4.0	93.5	71.8	110.0	46.8	122.2	405	20.3
0	acetate	4.0	145.8	75.3	110.0	47.1	123.0	387	32.1
0	phosphate	6.0	41.0	81.8	122.7	52.2	131.9	393	99.7
0	phosphate	7.0	39.0	84.8	124.7	52.6	132.3	420	104.0

[a] $T°$ is the reference temperature at which the intrinsic free energy $\Delta G°$ is equal to 0. [b] SSR is the sum of the square of the residuals.

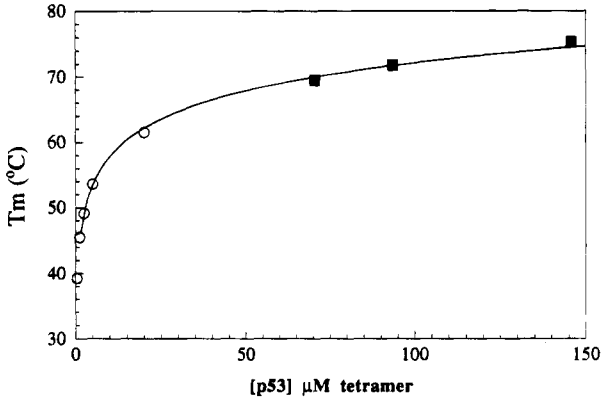

FIGURE 5: Unfolding transition temperature (T_m) of p53tet as a function of tetramer concentration. The open circles are from CD experiments; solid squares are DSC-determined data. For the CD data the T_m is estimated as the temperature at which the rate of change in the fraction unfolded with temperature is maximal. The solid line is the predicted dependence according to the two-state tetramer self-dissociating model.

Here $T°$ is the reference temperature, and by definition $\Delta G°$ is 0 at this temperature. It should be noted that $T°$ does not correspond to the transition temperature (T_m), which is defined as the peak maximum in the heat capacity function. Also, this temperature does not correspond to the temperature where the transition is half-completed (Freire, 1989).

To analyze DSC data, an expression for the average excess enthalpy function ($\langle\Delta H\rangle$) is needed (Freire & Biltonen, 1978). At any temperature, $\langle\Delta H\rangle$ for the p53tet tetrameric two-state system is given by

$$\langle\Delta H\rangle = F_U \Delta H°(T) \quad (9)$$

Here $\Delta H°(T)$ is the total unfolding enthalpy at temperature T. The excess heat capacity function that is measured by DSC is the temperature derivative of eq 9.

$$\langle\Delta C_p\rangle = \Delta H°(T)\frac{\partial F_U}{\partial T} + F_U \Delta C_p \quad (10)$$

In order to fit the calorimetric data, nonlinear least squares optimization of the experimental excess heat capacity was performed, utilizing the above expression after proper substitution. The analysis was conducted by solving for the roots of eq 6 numerically, as the exact formulation is complexed. It was found that the data could be adequately represented by the two-state tetramer self-dissociating model in which the only significantly populated states are the folded tetramer and unfolded monomers. The solid lines in Figures 2, 4, and 6 were calculated with this model and the thermodynamic parameters in Table 1. Inclusion of intermediate states did not significantly improve the fit of the data.

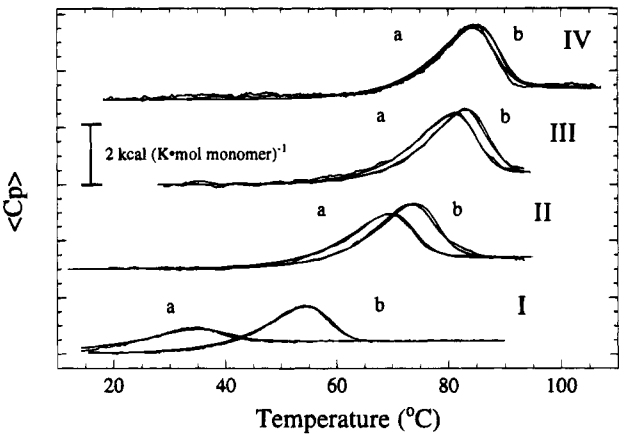

FIGURE 6: Excess heat capacity of p53tet as a function of pH and salt concentration. Excess heat capacity values have been offset by 2 kcal (K·mol of monomer)$^{-1}$ for ease of presentation. Experimental conditions are (Ia) 25 mM glycine at pH 3.0, (Ib) 25 mM glycine at pH 3.0 and 250 mM sodium chloride, (IIa) 25 mM sodium acetate at pH 4.0, (IIb) 25 mM sodium acetate at pH 4.0 and 250 mM sodium chloride, (IIIa) 25 mM sodium phosphate at pH 6.0, (IIIb) 25 mM sodium phosphate at pH 6.0 and 250 mM sodium chloride, (IVa) 25 mM sodium phosphate at pH 7.0, and (IVb) 25 mM sodium phosphate at pH 7.0 and 250 mM sodium chloride. Experimental values are shown along with their corresponding theoretically generated values obtained from the fitted parameters presented in Table 1.

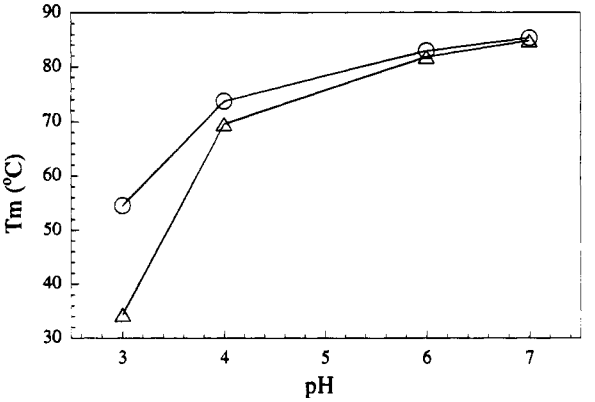

FIGURE 7: Transition temperature of p53tet as a function of pH and salt concentration. The triangles represent the values in the absence of salt while the circles give the transition temperature in the presence of 250 mM sodium chloride. The values are taken from Table 1 which describes the experimental conditions.

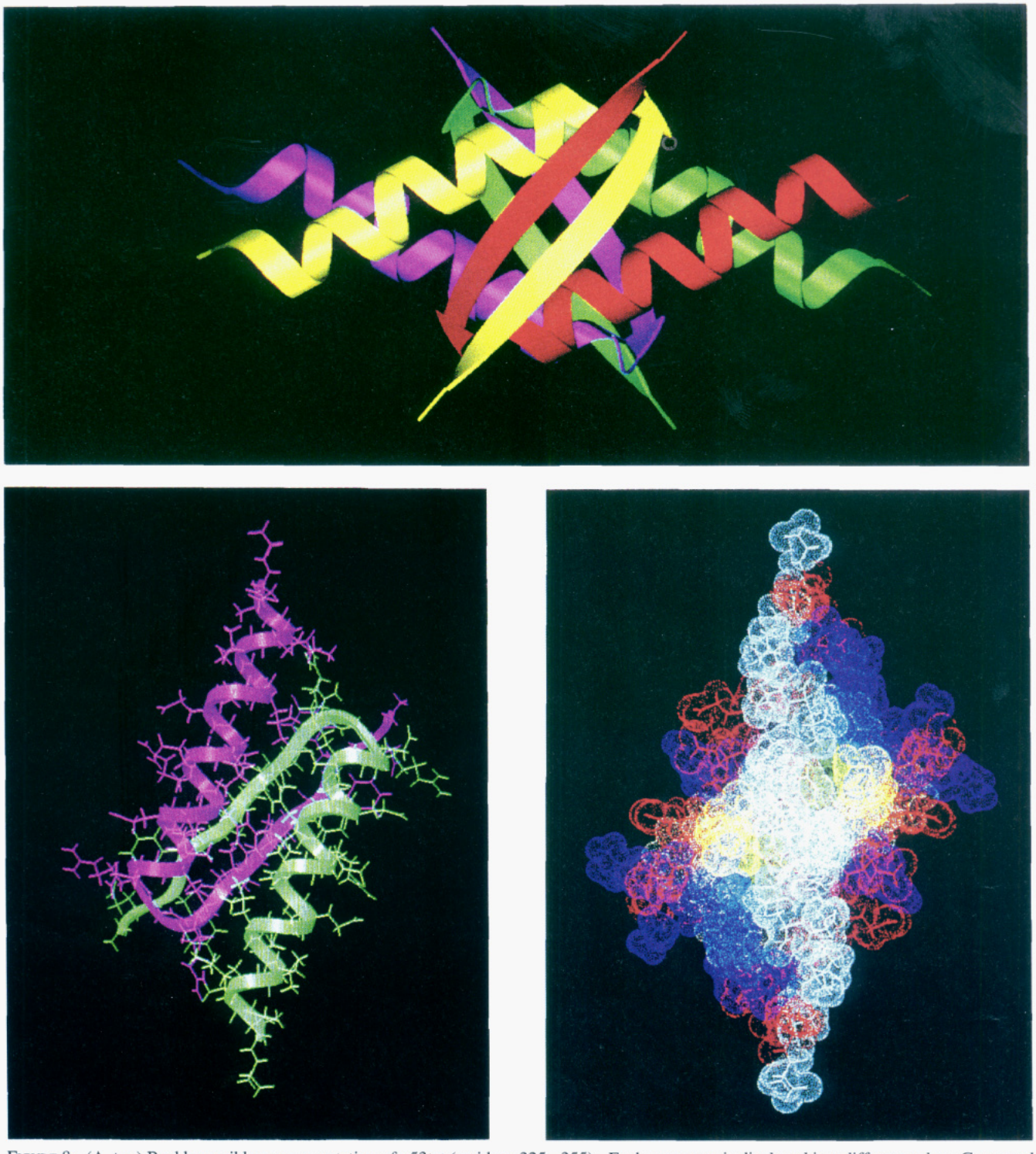

FIGURE 8: (A, top) Backbone ribbon representation of p53tet (residues 325−355). Each monomer is displayed in a different color. Generated with SETOR (Evans, 1993), adapted from Lee et al. (1994). (B, bottom left) View of the green/purple dimer (rotated 55° relative to panel A) as "seen" by the yellow/red dimer. Generated with InsightII. (C, bottom right) Van der Waals surface of the green/purple dimer displayed in the same view as in panel B but with the side chains coded for hydrophobicity. White residues are hydrophobic, yellow is methionine, red are acidic, and blue are basic. The extended white surface between dimers is evident. Generated with Insight II.

The variable concentration CD data shown in Figure 4 display unfolding data down to a concentration of 0.5 μM tetramer. The figure shows the experimentally determined values along with the calculated curves generated from parameters obtained calorimetrically at higher concentrations under the same solution conditions (Table 1). At $T°$, the temperature at which the intrinsic free energy is 0 (110.3 °C), the average calorimetric value for $\Delta H°$ at pH 4.0 in sodium acetate is 46.7 kcal (mol of monomer)$^{-1}$ with a $\Delta S°$ change of 121.9 cal (K·mol of monomer)$^{-1}$ and a ΔC_p of 397 cal (K·mol of monomer)$^{-1}$. From Figures 2 and 4 it is evident that the model described above gives an accurate description of the concentration dependence of the unfolding transition. This information is summarized in Figure 5 where the transition temperature (T_m) is plotted versus the tetramer concentration of p53tet. As shown in the figure, the parameters in Table 1 accurately account for the 35 °C variation in transition temperature observed within the concentration range studied.

Table 2: Calculated Changes in Accessible Surface Area (per Monomer) for p53tet Unfolding

	ΔASA_{total} (Å^2)	ΔASA_{ap} (Å^2)	ΔASA_{pol} (Å^2)	$\Delta C_p(25)$ [cal (K·mol of monomer)$^{-1}$]	$\Delta H(60)$ [cal (mol of monomer)$^{-1}$]
subunit interface dissociation	1616	1152	464	386	4850
unfolding of isolated monomer	1266	750	516	195	9900
total for unfolding of tetramerization domain	2882	1902	980	581	14750

In order to explore the pH and salt dependence of the unfolding transition, experiments were also conducted at a number of different salt and buffer conditions (Figure 6, Table 1). As shown in the figure, a decrease in pH significantly destabilized the tetramer, lowering the transition temperature by about 35 °C between pH 7 and pH 3. At all pH values, however, the two-state tetramer self-dissociating model was adequate to account for the experimental data, indicating that at these lower pH conditions the molecule was still in its tetrameric form proceeding to unfolded monomers as the transition occurs. At increased salt concentration the tetramer was stabilized significantly at low pH values; however, at pH values close to neutral the effect of salt concentration was insignificant. Figure 7 displays the pH dependence of the transition temperature at two salt concentrations.

Structural Thermodynamic Calculations. The NMR structure of p53tet has been recently determined (Lee et al., 1994). The structure is a dimer of dimers with three mutually perpendicular axes of 2-fold symmetry rather than 4-fold symmetry. Residues 326−334 are in a β-strand conformation while residues 337−354 form a relatively stable α-helix. Residues 303−324 and 356−366 are apparently unstructured as judged by their NMR parameters (Lee et al., 1994). The β-strands of each p53tet peptide subunit are paired with a second strand forming two separate but identical two-stranded β-sheets establishing two dimers. The helices form a four-helix bundle in an "X" pattern (Harris et al., 1994) as shown in Figure 8A. Each dimeric half forms a compact unit having helices packed antiparallel to one another and with the helical axis of one roughly parallel to the β-strand of the other (Figure 8A,B). Figure 8C demonstrates the extended hydrophobic surface (in white) which forms the interface between the two dimers.

The extent of polar and apolar surfaces that are buried from the solvent is a major determinant of the stability of the native state. Protein-asscessible surface area calculations were analyzed as previously described (Murphy et al., 1992) using the implementation of Lee and Richard's algorithm (Lee & Richards, 1971) in the program ACCESS (Scott R. Presnell, University of California) with a probe radius of 1.4 Å and a slice width of 0.25 Å. These parameters are summarized in Table 2. It is clear from this table that approximately 58% of the total buried surface area resides at the interface between subunits. Also it must be noted that most of the surface buried at the interface (70%) is apolar, indicating that the driving force for tetramerization is hydrophobic. In contrast, the surface area buried by an isolated monomer is only 60% apolar. Proportionally, the tetramerization domain buries a larger fraction of apolar surface than most globular proteins (~58%). Under the conditions studied here, p53tet monomers or even dimers are not thermodynamically stable relative to the tetramer and therefore do not become populated. They probably exist in only a transient form and rapidly disappear as a result of the tetramerization reaction. According to the calorimetric data, the total free energy of stabilization at 25 °C is 6.5 kcal (mol of monomer)$^{-1}$. Within this total, the entropic contribution of tetramerization due to solvent reorganization (hydrophobic effect) to the free energy of stabilization is on the order of 30 kcal (mol of monomer)$^{-1}$ at 25 °C. This result emphasizes the role of hydrophobic interactions in the stabilization of p53tet.

Table 2 also summarizes the expected contributions of the tetramerization domain to $\Delta C_p(25)$ and $\Delta H(60)$ calculated as described previously (Murphy et al., 1992; Murphy & Freire, 1992; Xie & Freire, 1994a,b). The calculated change in the enthalpy of unfolding at 60 °C for the tetramerization domain alone (residues 325−355) is noticeably smaller than the experimental value extrapolated to that temperature [26 kcal (mol of monomer)$^{-1}$] obtained for the 303−366 fragment. Since this discrepancy is larger than the expected error arising from the structural parameterization, it probably arises from some residual structure in the additional 32 amino acids per monomer present in the sample studied. If, for example, only three contiguous amino acids immediately adjacent to the putative N and C terminus are considered to be ordered, the expected enthalpy change will increase to about 22 kcal (mol of monomer)$^{-1}$, in better agreement with the experimental result. This possibility is strengthened by the analysis of the CD data which indicates a somewhat larger amount of secondary structure than that corresponding to the tetramerization domain alone.

CONCLUSIONS

In this paper we have demonstrated that the thermal unfolding of p53tet is a two-state process in which the folded tetramer unfolds cooperatively into unfolded monomers. Under all conditions studied the concentration of intermediate species consisting of folded dimers or monomers could not be detected calorimetrically. Also, the CD data are consistent with the presence of only two significantly populated states. This description is consistent with the observation that the majority of interfacial contacts in the tetramer are hydrophobic, making isolated dimeric or monomeric structures less stable. It must be noted, however, that a relative destabilization of the tetramerization interface by mutations or solvent conditions might, in certain situations, stabilize isolated dimers relative to the tetramer (Waterman et al., 1995). The hydrophobic effect appears to be the major stabilizing force of the tetramerization domain.

REFERENCES

Bargonetti, J., Manfredi, J. J., Chen, X., Marshak, D. R., & Prives, C. (1993) *Genes Dev.*, 2565−2574.

Cho, Y., Gorina, S., Jeffery, P. D., & Pavletich, N. P. (1994) *Science 265*, 346−355.

Clore, G. M., Omichinski, J. G., Sakaguchi, K., Zambrano, N., Sakamoto, H., Appella, E., & Gronenborn, A. M. (1994) *Science 265*, 386−391.

Donehower, L. A., & Bradley, A. (1993) *Biochim. Biophys. Acta 1155*, 181.

Evans, S. V. (1993) *J. Mol. Graphics 11*, 134−138.
Freire, E. (1989) *Comments Mol. Cell. Biophys. 6*, 123−140.
Freire, E. (1994) *Methods Enzymol. 240*, 502−568.
Freire, E., & Biltonen, R. L. (1978) *Biopolymers 17*, 463−479.
Gill, S. C., & von Hippel, P. H. (1989) *Anal. Biochem. 182*, 319−326.
Gomez, J., Hilser, V. J., Xie, D., & Freire, E. (1995) *Proteins* (in press).
Halazonetis, T. D., & Kandil, A. N. (1993) *EMBO J. 12*, 5057−5064.
Harris, C. C. (1993) *Science 262*, 1980.
Harris, N. L., Presnell, S. R., & Cohen, F. E. (1994) *J. Mol. Biol. 236*, 1356−1368.
Hollstein, M., Sidransky, D., Vogelstein, B., & Harris, C. C. (1991) *Science 253*, 49−53.
Hupp, T. R., Meek, D. W., Midgely, C. A., & Lane, D. P. (1992) *Cell 71*, 875−886.
Lane, D. P. (1992) *Nature 358*, 15.
Lee, B., & Richards, F. M. (1971) *J. Mol. Biol. 55*, 379−400.
Lee, W. T., Harvey, T. S., Yin, Y., Yau, P., Litchfield, D., & Arrowsmith, C. H. (1994) *Nature Struct. Biol. 1*, 877−890.
Levine, A. J., Mommand, J., & Finlay, C. A. (1991) *Nature 351*, 453−456.
Makhatadze, G. I., & Privalov, P. L. (1990) *J. Mol. Biol. 213*, 375−384.
Montgomery, D., Jordan, R., McMacken, R., & Freire, E. (1993) *J. Mol. Biol. 232*, 680−692.
Murphy, K. P., & Freire, E. (1992) *Adv. Protein Chem. 43*, 313−361.
Murphy, K. P., Bhakuni, V., Xie, D., & Freire, E. (1992) *J. Mol. Biol. 227*, 293−306.
Pavletich, N., Chambers, K. A., & Pabo, C. O. (1993) *Genes Dev. 7*, 2556−2564.
Studier, F. W. (1991) *J. Mol. Biol. 219*, 37−44.
Sturzbecher, H. W., Brain, R., Addison, C., Rudge, K., Remm, M., Grimaldi, M., Keenan, E., & Jenkins, J. R. (1992) *Oncogene 7*, 1513−1523.
Thompson, K. S., Vinson, C. R., & Freire, E. (1993) *Biochemistry 32*, 5491−5496.
Unger, T., Nau, M. M., Segal, S., & Minna, J. D. (1992) *EMBO J. 4*, 1383−1390.
Vogelstein, B., & Kuntzler, K. W. (1992) *Cell 70*, 523−526.
Waterman, J. L. F., Shenk, J. L., & Halazonetis, T. D. (1995) *EMBO J. 14*, 512−519.
Xie, D., & Freire, E. (1994a) *Proteins: Struct., Funct., Genet. 19*, 291−301.
Xie, D., & Freire, E. (1994b) *J. Mol. Biol. 242*, 62−80.
Xie, D., Fox, R., & Freire, E. (1994) *Protein Sci. 3*, 2175−2184.

BI950140Z